

## Magnetic and Martensitic Transitions in $\text{Ni}_2\text{Mn}_{1+x}\text{Sn}_{1-x}$ Alloys

S. Chatterjee<sup>a</sup> and S. Majumdar<sup>b</sup>

Department of Solid State Physics, Indian Association for the Cultivation of Science,

2A & B Raja S. C. Mullick Road, Jadavpur, Kolkata 700 032, India

<sup>a</sup>sspsc@iacs.res.in, <sup>b</sup>sspsm2@iacs.res.in

**Keywords:** Magnetic ground state, magnetoresistance, field arrested state.

**Abstract.** The magnetic phase diagram of  $\text{Ni}_2\text{Mn}_{1+x}\text{Sn}_{1-x}$  based ferromagnetic (FM) shape memory alloys for varied concentrations of  $x$  have been studied. With increasing concentration of Mn, the FM Curie temperature ( $T_C$ ) decreases, while the martensitic transition temperature ( $T_M$ ) goes higher. For  $x = 0.44$  and  $0.48$ ,  $T_M$  is close to the onset of ferromagnetism, and two distinct magnetic transitions are observed corresponding to the  $T_C$ 's of the FM phases of martensite and austenite respectively. The isothermal magnetization at 5 K indicates saturating behaviour at high fields and the saturation moment drops linearly with  $x$ . The samples show reasonably large negative magnetoresistance around  $T_M$ , however the magnitude drops with increasing  $x$ . The magnetoresistance is found to be highly irreversible with respect to the applied magnetic field and field induced arrested state is observed for all the FM samples studied around the first order martensitic transition. The present investigation clearly indicates complex magnetic ground state of the  $\text{Ni}_2\text{Mn}_{1+x}\text{Sn}_{1-x}$  samples with competing magnetic interactions.

### Introduction

In recent times,  $\text{Ni}_2\text{Mn}_{1+x}\text{Z}_{1-x}$  ( $Z = \text{Sn}, \text{Sb}, \text{In}$ ) type ferromagnetic shape memory alloys (FSMAs) are emerging as the potential alternative for the familiar Ni-Mn-Ga system of alloys [1-5]. The former compositions are less brittle and less toxic than the Ni-Mn-Ga alloys, and therefore found to be suitable for practical applications. They provide fascinating electronic and magnetic properties, which include phase coexistence, metastability, field induced reverse transition, glassy magnetic phase, magnetic exchange anisotropy, kinetically arrested state, inverse magnetocaloric effect etc.[6-11]. It has been observed that the magnetic, electronic and structural properties of these alloys are very closely interlinked. One big advantage in  $\text{Ni}_2\text{Mn}_{1+x}\text{Z}_{1-x}$  is that the alloys exist over a wide range of Mn concentration and therefore provide an opportunity to investigate the origin of their properties through doping studies.

In the present work, we have investigated several Ni-Mn-Sn based samples with formulation,  $\text{Ni}_2\text{Mn}_{1+x}\text{Sn}_{1-x}$  ( $x = 0.36, 0.40, 0.44, 0.48, 0.52$ ). It has been already reported that the martensitic transition temperature ( $T_M$ ) of the alloys increases with increasing  $x$ , while the ferromagnetic Curie point ( $T_C$ ) decreases. [6] The present work brings out interesting trend in the evolution of various magnetic and transport properties with increasing Mn concentration in the sample.

### Experimental Details

The polycrystalline sample of compositions  $\text{Ni}_2\text{Mn}_{1+x}\text{Sn}_{1-x}$  ( $x = 0.36, 0.40, 0.44, 0.48$  and  $0.52$ ) were prepared by argon arc melting the constituent elements (purity 99.9% or above). The ingots were homogenized in a sealed evacuated quartz tube at  $900^\circ\text{C}$  for 42 hours, followed by a quenching in ice water. The room temperature powder x-ray diffraction patterns ( $\text{Cu K}\alpha$ ) confirm that  $x = 0.36, 0.40$  and  $0.44$  materials are single-phase alloys with cubic Heusler ( $L2_1$ ) structure, while  $x = 0.48$  material is found to have both cubic ( $L2_1$ ) and orthorhombic four-layered ( $4O$ ) structures. This is due to the fact that  $T_M$  for the former alloys are well below the room temperature, while for  $x = 0.48$  alloy,  $T_M$  is around room temperature and as a result it shows a mixture of cubic austenite and

orthorhombic martensite phases. For  $x = 0.52$  alloy with  $T_M$  well above room temperature, we only observe orthorhombic martensite phase in the x-ray diffraction pattern.

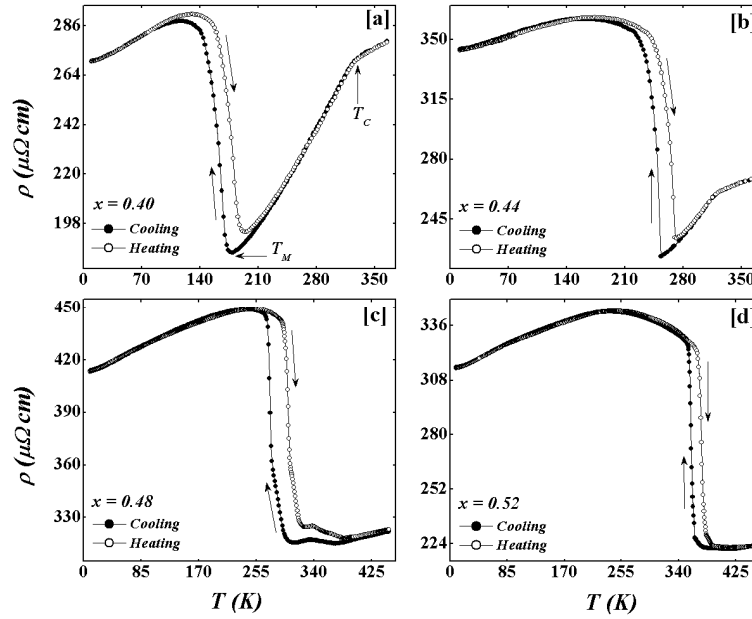


**Fig.1:** Resistivity as a function of temperature for the  $\text{Ni}_2\text{Mn}_{1+x}\text{Sn}_{1-x}$  alloys. For each composition, both heating and cooling data are depicted in the plot.

The resistivity ( $\rho$ ) of the samples was measured by standard four probe technique in the temperature ( $T$ ) range between 5 and 460 K using both liquid nitrogen cryostat and a commercial closed cycle refrigerator. Magnetoresistance was measured using a cryogen free high magnetic field device from Cryogenic Ltd., UK. The magnetization ( $M$ ) was measured by Quantum Design SQUID magnetometer (MPMS 6, Ever-cool model) and commercial cryogen free vibrating sample magnetometer from Cryogenic Ltd., UK in the temperature range 5-300 K. A homemade mutual induction type setup was used to measure the ac susceptibility ( $\chi'_{ac}$ ) down to liquid nitrogen temperature.

## Results and Discussion

Fig. 1 shows the  $\rho$  versus  $T$  data for different compositions for both cooling and heating sequences. All the samples show clear anomaly related to the martensitic transition (MT), which is associated with the thermal hysteresis. The martensitic start temperature,  $T_M$  is indicated by an arrow in fig. 1a for  $x = 0.40$  sample only. We observe that  $T_M$  is extremely sensitive with the composition of the alloy: for  $x$  changing from 0.36 to 0.52,  $T_M$  changes from 110 K to 375 K. Apart from MT, a clear signature of change in slope due to paramagnetic (PM) to ferromagnetic (FM) transition is observed, which has been indicated by  $T_C$  in fig 1a.

In order to estimate  $T_M$  and  $T_C$  for wide range of compositions, we have used dc magnetization ( $M$ ) and ac susceptibility data along with  $\rho(T)$  data. Fig. 2 shows the  $M$  versus  $T$  data for different samples up to maximum temperature of 300 K. The data have been recorded for both field-cooled cooling (FCC) and field-cooled heating (FCH) protocols in presence of 100 Oe of applied magnetic field ( $H$ ). The MT is clearly identified by the characteristic thermal hysteresis and the corresponding  $T$  matches well with the anomaly in  $\rho(T)$ . Since  $M(T)$  measurements are restricted to the maximum  $T$  of 300 K, the full thermal hysteresis due to MT is only visible for the  $x = 0.40$  and 0.44 samples. A partial (minor) loop is seen for the 0.48 sample, while no loop is present for the  $x = 0.52$  data as the MT for the sample is well above 300 K. This is supported by the observation of pure martensitic orthorhombic phase in the x-ray diffraction pattern at room temperature for that particular sample.

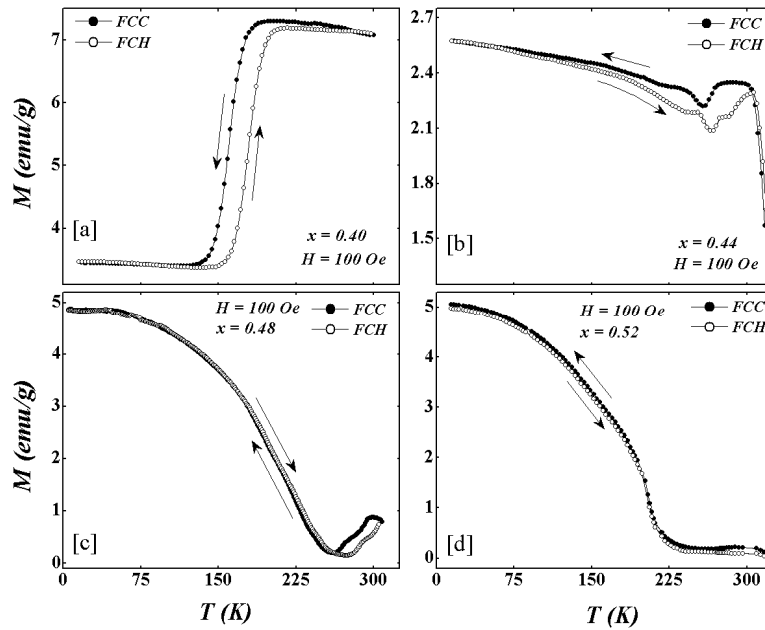


**Fig.2:** Magnetization ( $M$ ) as a function of temperature for the  $\text{Ni}_2\text{Mn}_{1+x}\text{Sn}_{1-x}$  alloys recorded at an applied field of 100 Oe in FCH and FCC condition.

If one looks carefully on the  $M(T)$  behaviour of  $x = 0.48$  sample, a dip is observed within the region of MT. Similar dip has been observed in some other FSMA's within the region of MT [5, 12]. This has been interpreted due to the existence of two critical temperatures corresponding to the FM phases of martensite and austenite. It might happen in certain situations, particularly when  $T_M$  is close to the  $T_C$  of the austenite phase ( $T_{CA}$ ), the martensite  $T_C$  ( $T_{CM}$ ) may separate out from  $T_{CA}$ .

We show  $\chi'_{ac}(T)$  data up to 400 K in fig. 3a for  $x = 0.48$  sample. Two anomalies are clearly visible in the data, which are actually separated by the thermal hysteresis region of the MT. With decreasing  $T$ , the sample shows sharp rise in  $\chi'_{ac}$  around 330 K, which indicates the long range FM order in the austenite phase with  $T_{CA} = 330$  K. Further lowering in  $T$  results the MT, where  $\chi'_{ac}$  falls drastically. It again shows the peak like anomaly around 250 K, which can be identified as the  $T_{CM}$  of the martensite phase. The resistivity data show multiple anomalies for the sample around the MT.

In order to ascertain the true significance of  $T_{CA}$  and  $T_{CM}$ , we measured isothermal  $M$  versus  $H$  as shown in fig. 3b for  $x = 0.48$  sample. We observe a clear non-monotonic change in the behaviour of the  $M$ - $H$  curves with  $T$ . At 5 K, the sample shows FM behaviour with the highest saturation moment. Similar FM nature is seen at 307 K (below  $T_{CA}$  but above  $T_M$ ) and 206 K (below  $T_{CM}$ ), although with reduced values of the saturation moment. However, the nature of the curve is completely different at 276 K, which is between  $T_{CM}$  and  $T_M$ . Here the moment is much lower than the other curves, and it does not show a rising part at low values of  $H$ . In addition, a strong field-hysteresis is observed, which is not very apparent at other isotherms. It suggests that the sample is not ferromagnetic at 276 K. The sample presumably orders ferromagnetically at  $T_{CA}$ , loses its ferromagnetism below  $T_M$  (becomes paramagnetic) and then again second ferromagnetic phase develops below  $T_{CM}$ . This is an example of *re-entrant ferromagnetism*, and we observe two  $T_C$ 's [5]. However, one should remember that at 276 K, the sample is in a metastable phase. The observed field hysteresis might indicate the field induced transition to an FM phase by the application of  $H$ . Considering the fact that Ni-Mn-Sn alloys show reverse structural transition (martensite to austenite) under  $H$  [9], the applied field at 276 K might cause regeneration of the austenitic FM phase.

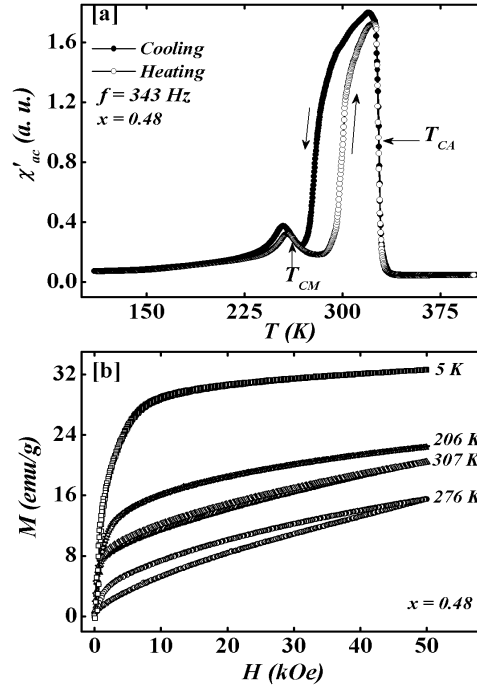


**Fig.3:** [a] Real part of ac susceptibility ( $\chi'_{ac}$ ) is plotted as a function of temperature ( $T$ ) at 343 Hz of applied frequency of ac signal for  $x=0.48$  sample. [b] Isothermal magnetization ( $M$ ) is plotted as a function of applied magnetic field at different constant temperature for  $x=0.48$  sample.

Now let us look at the magnetoresistance ( $MR = [\rho(H) - \rho(0)] / \rho(0)$ ) data recorded for different samples (see fig. 4). In fig. 4 we have shown MR of four samples, measured at  $T$  lying close to the centre of their respective MT region, where the MR is supposed to be highest. In practice the measurement temperatures were chosen to be the mean temperatures of the two end point of the thermal hysteresis loops in  $\rho(T)$ . Clearly all the samples show very similar MR behaviour, although with different values of the absolute magnitude. The value of MR at the centre of the MT are -26%, -16%, -13%, -4% for  $x = 0.36, 0.40, 0.44$  and  $0.48$  respectively for applied field of 50 kOe recorded on the heating cycle. The observed MR is found to be highly irreversible with respect to the applied field, and even if the field is removed, the samples do not return back to their virgin zero field value of  $\rho$ . This is a clear indication of field induced arrest around the martensitic type magneto-structural transition [9].

The noteworthy point in the present measurements is that the absolute magnitude of MR drops systematically with the increasing Mn concentration of the sample. The phase diagram for the  $Ni_2Mn_{1+x}Sn_{1-x}$  alloys are shown in fig. 5a. As evident, with increasing  $x$  (and hence Mn concentration)  $T_M$  increases linearly, and simultaneously absolute magnitude of the MR varies almost linearly. In the phase diagram, two FM transition temperatures,  $T_{CA}$  and  $T_{CM}$  are shown for the samples. For  $x = 0.36$  to  $0.40$ , only one single  $T_C$  is observed, and it is found to be almost independent of concentration. However, for  $x = 0.44$  and  $0.48$  signature of two distinct  $T_C$ 's are observed. The observation of two  $T_C$ 's is due to the fact that FM phase becomes unstable in the martensite phase due to lower crystallographic symmetry and sample transforms into paramagnetic phase. As the temperature is further lowered, the FM phase wins over the thermal fluctuation and a second  $T_C$  is observed. For  $x = 0.36$  and  $x = 0.40$  samples,  $T_M$  is already low, and therefore the two FM phases may overlap.

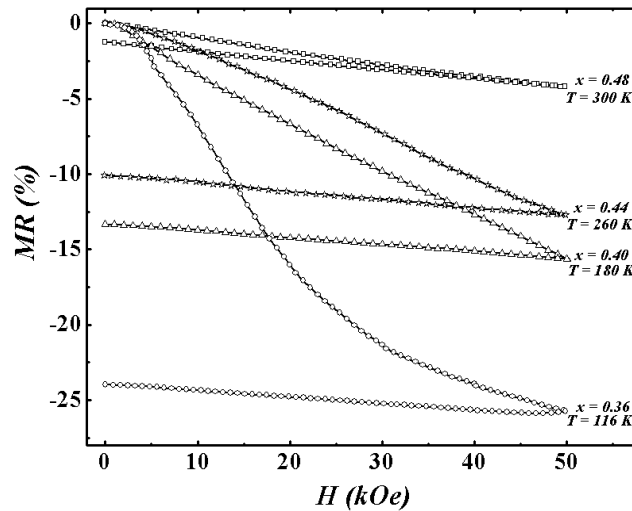


**Fig.4:** Magnetoresistance is plotted as a function of temperature for  $x=0.36, 0.40, 0.44, 0.48, 0.52$  alloys at different constant temperature.

The gradual change in  $T_M$  with  $x$  is presumably related to the change in the ratio of electron concentration to the number of atoms ( $e/a$  ratio) as observed in Ni-Mn-Ga system of alloys [13]. The increasing  $e/a$  ratio with the increasing concentration is expected to bring structural instability and as a result  $T_M$  will increase. The magnitude of MR, measured at the respective mid-point of the MT, decreases with  $x$ . This can naively be ascribed to the increase of  $T_M$  with  $x$ , because MR is expected to decrease with  $T$  due to enhanced thermal fluctuations. However, the effect can be subtle, as addition of excess Mn at the Sn site actually aligns antiferromagnetically with original Mn atoms. The MR observed in  $\text{Ni}_2\text{Mn}_{1+x}\text{Sn}_{1-x}$  alloys is related to the field induced reverse transition [8], and increasing antiferromagnetic (AFM) correlation with  $x$  may alter the field-induced transition. A recent polarized neutron scattering investigations on  $\text{Ni}_2\text{Mn}_{1+x}\text{Z}_{1-x}$  ( $Z = \text{Sn}, \text{Sb}$ ) confirms the existence of AFM state in the otherwise FM alloys. [14]

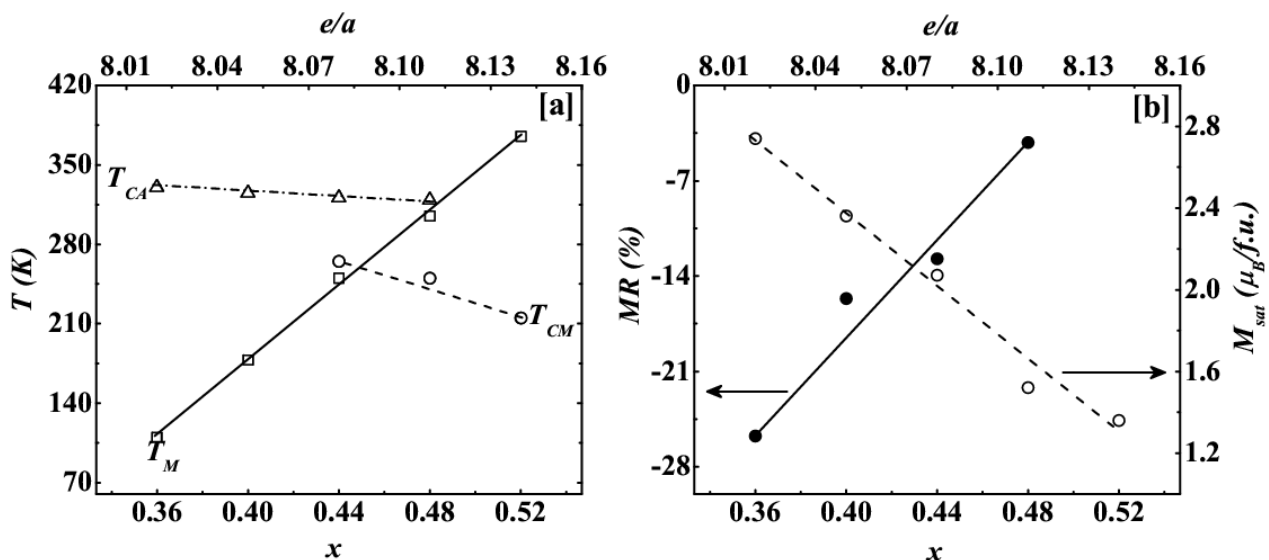


**Fig.5:** [a]  $T_M$ ,  $T_{CA}$ ,  $T_{CM}$  and [b] MR,  $M_{sat}$  are plotted as a function of excess Mn concentration (here  $x$ ) and also as a function of  $e/a$  ratio.

The existence of AFM correlations in  $\text{Ni}_2\text{Mn}_{1+x}\text{Sn}_{1-x}$  alloys is further supported by the variation of saturation moment ( $M_{sat}$ ), which has been obtained from isothermal magnetization measurement at 5 K up to 50 kOe of field. The value of  $M_{sat}$  decreases linearly with  $x$ , indicating the existence of antiparallel spins arrangements in the system.

## Conclusion

We observe a systematic variation of the magnetic and transport properties of  $\text{Ni}_2\text{Mn}_{1+x}\text{Sn}_{1-x}$  alloys with  $x$ . For certain concentration, we observe re-entrant FM phase, which occurs across the MT in those samples. All the samples show very similar open ended MR versus  $H$  behaviour within the region of MT, which is closely connected to the irreversible nature of the field induced transition, reported earlier in various Ni-Mn-Z alloys [8, 9]. The present study strengthens the view of the role of electron concentration in determining the structural properties of the shape memory alloys. In addition, it once again indicates the existence of AFM correlations in the excess Mn doped alloys, which gives rise to fascinating effect like reentrant ferromagnetism and MR anomalies.

## Acknowledgement

The present work is financially supported by CSIR, India.

## References

- [1] Y. Sutou, Y. Imano, N. Koeda, T. Omori, R. Kainuma, K. Ishida, and K. Oikawa, Appl. Phys. Lett. **85**, 4358 (2004).
- [2] R. Kainuma, Y. Imano, W. Ito, Y. Sutou, H. Morito, S. Okamoto, O. Kitakami, K. Oikawa, A. Fujita, T. Kanomata, and K. Ishida, Nature **439**, 957 (2006).
- [3] L. Mañosa, X. Moya, A. Planes, T. Krenke, M. Acet, E.F. Wassermann, Materials Science and Engineering A **481–482**, 49 (2008).
- [4] T. Krenke, E. Duman, M. Acet, E. F. Wassermann, X. Moya, L. Mañosa, A. Planes, E. Suard, B. Ouladdiaf, Phys. Rev. B **75**, 104414 (2007).
- [5] T. Krenke, M. Acet, E. F. Wassermann, X. Moya, L. Mañosa, and A. Planes, Phys. Rev. B **72**, 014412 (2005).
- [6] K. Koyama, K. Watanabe, T. Kanomata, R. Kainuma, K. Oikawa, and K. Ishida, Appl. Phys. Lett. **88**, 132505 (2006).
- [7] S. Chatterjee, S. Giri, S. Majumdar, A. K. Deb, S. K. De, and V. Hardy, J. Phys.: Condens. Matter **19**, 346213 (2007).
- [8] V. K. Sharma, M. K. Chattopadhyay, and S. B. Roy, Phys. Rev. B **76**, 140401(R) (2007).
- [9] S. Chatterjee, S. Giri, S. Majumdar, and S. K. De, Phys. Rev. B **77**, 012404 (2008).
- [10] M. Khan, I. Dubenko, S. Stadler, and N. Ali, Appl. Phys. Lett. **91**, 072510 (2007).
- [11] S. Chatterjee, S. Giri, S. K. De, and S. Majumdar, Phys. Rev. B **79**, 092410 (2009).
- [12] V. D. Buchelnikov, P. Entel, S. V. Taskaev, V. V. Sokolovskiy, A. Hucht, M. Ogura, H. Akai, M. E. Gruner, and S. K. Nayak, Phys. Rev. B **78** 184427 (2008).
- [13] V. A. Chernenko, Scripta Materialia **40**, 523 (1999).
- [14] S. Aksoy, M. Acet, P. P. Deen, L. Mañosa, and A. Planes, Phys. Rev. B **79**, 212401 (2009).